Supporting Information

Electrochemical activation of graphene at low temperature: the synthesis of three-dimensional nanoarchitectures for high performance supercapacitor and capacitive deionization

Mohamed Zoromba[1,2], Mohamed Abdel-Aziz[1,3], Mohamed Bassyouni[1, 4], Saud Gutub[5], Denisa Demko[6], Amr Abdelkader[6,7]*

[1]Chemical and Materials Engineering Department, King Abdulaziz University, Rabigh 21911, Saudi Arabia

[2]Department of Chemistry, Faculty of Science, Port Said University, Port Said, Egypt.

[3]Chemical Engineering Department, Faculty of Engineering, Alexandria University, Alexandria, Egypt

[4]Department of Chemical Engineering, Higher Technological Institute, Tenth of Ramdan City, Egypt

[5]Civil Engineering Department, King Abdulaziz University, Rabigh 21911, Saudi Arabia

[6]Department of Engineering, University of Cambridge, Cambridge, CB3 0FA, UK

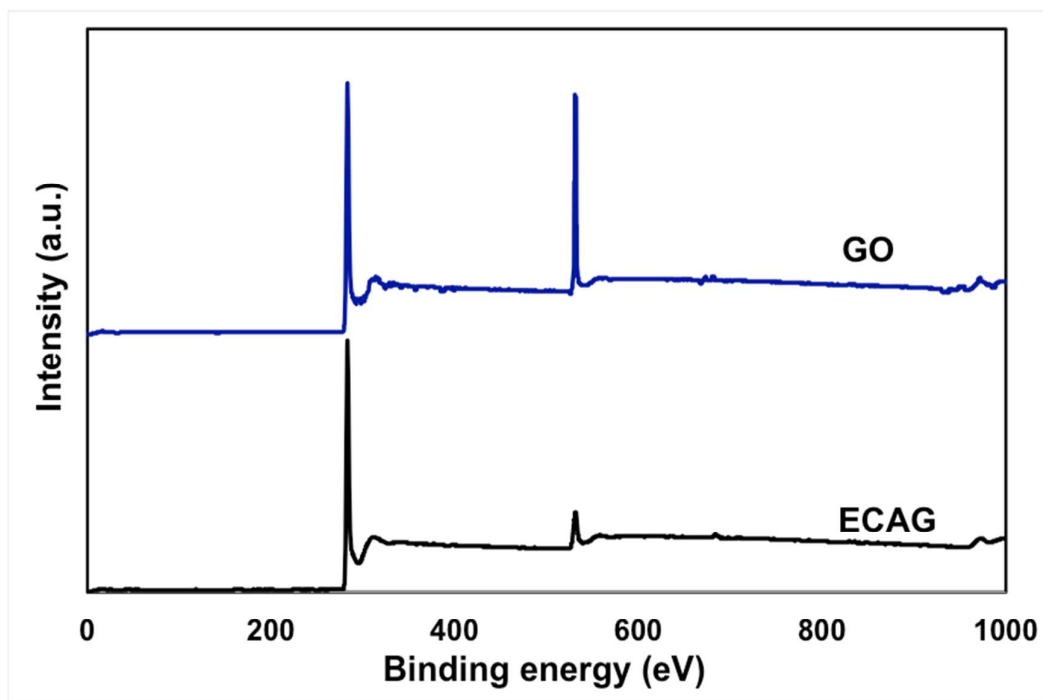[7]National Graphene Institute (NGI), University of Manchester, Booth Street East, Manchester, M13 9QS, UK

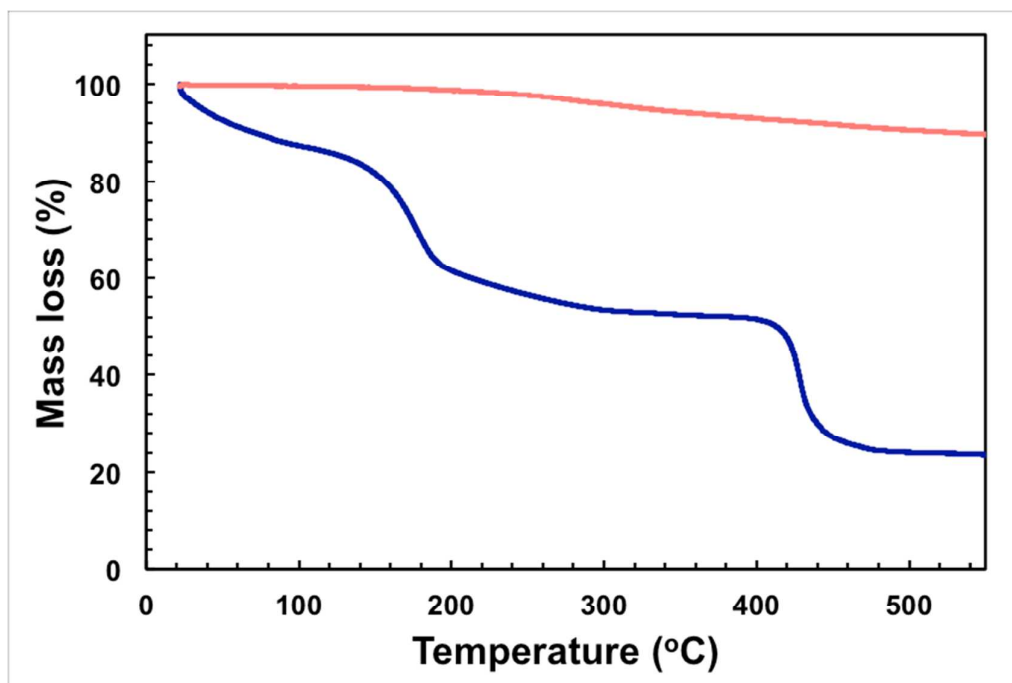*Corresponding author. Tel.: +441223 748349, Fax: +44 - 1223 – 748348, = *E-mail address: aa494@cam.ac.uk

10 Pages
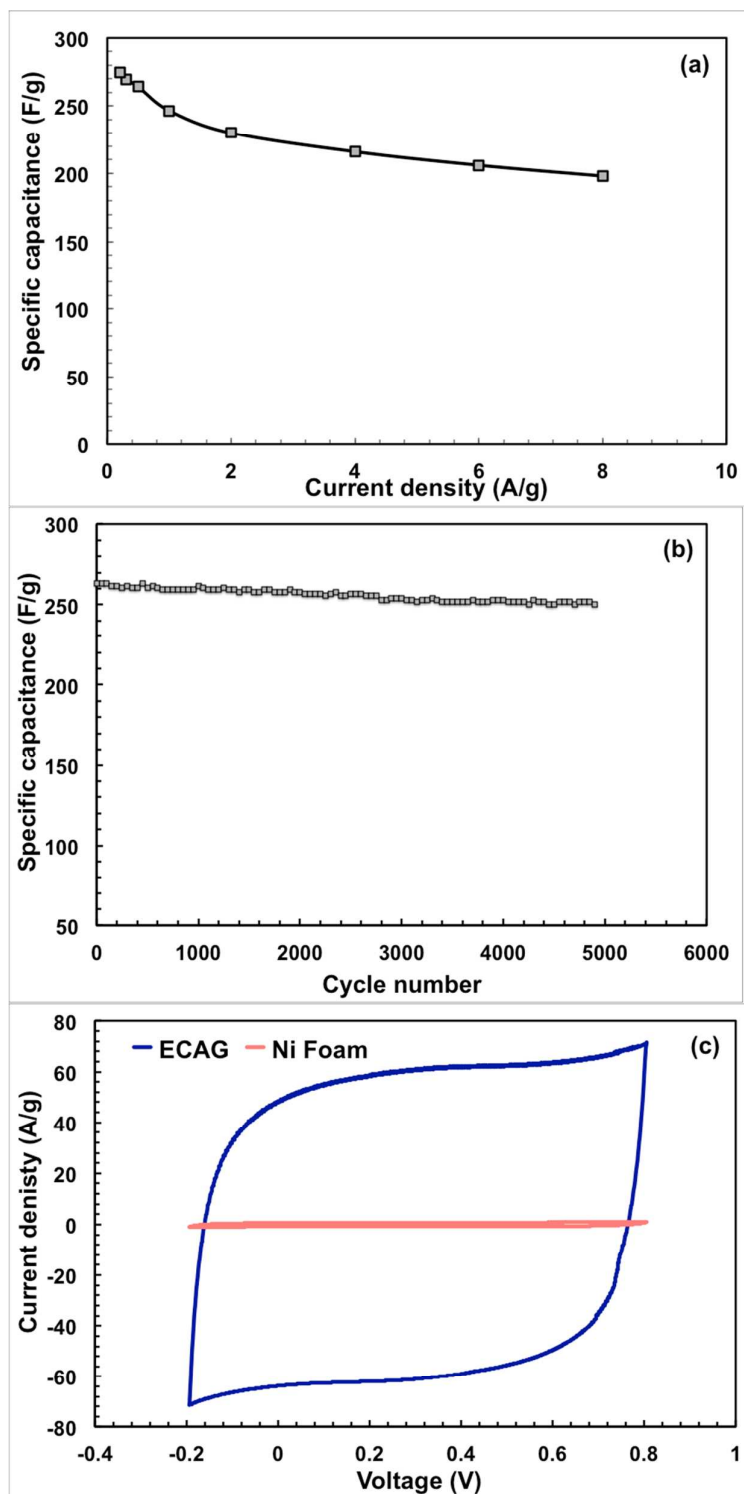**5 Figures**
2 Tables

Figure S1. XPS survey spectra of the GO and the ECAG. The intensity of the O1s peak at ~531 eV significantly reduced due to the removal of the oxygen groups.


Figure S2. Thermal gravimetric curve for the GO (blue) and the ECAG (red) showing the stability of the sample after the electrochemical treatment due to the removal of the oxygen functional groups.

Figure S3. (a) The change of the specific capacitance as a function of the current density of the supercapacitor symmetrical device made from 2 ECAG electrodes in 6 M KOH solution. (b) Cycle life stability of the symmetrical device in 6 M KOH solution, (c) CV measured for a 2 symmetrical supercapacitor devices fabricated form Ni foam and ECAG electrodes. The pseudocapacitance from the Ni foam is negligible as compare to the ECAG electrode.

Further analysis of the electrosorption ion removal process
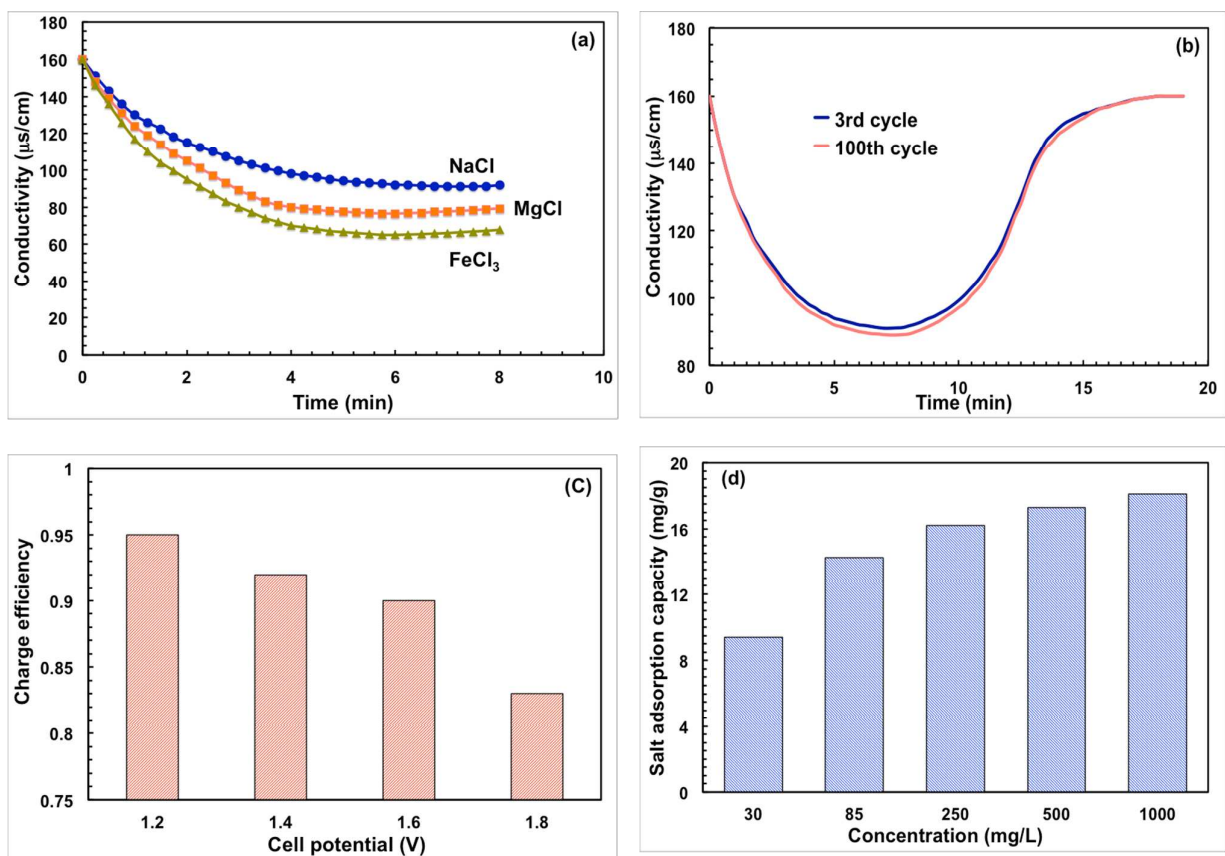
Figure S4. (a) Comparison of the change in the conductivity with time for different types of salts. (b) The electrosorption curve measured for the DCI device with ECAG electrode after 3 and 100 cycles, confirming the stability of the electrode (c) Equilibrium charge efficacy as a function of the applied potential (d) Equilibrium salt adsorption capacity as a function of the initial concentration of the NaCl solution**.**

Argon gas inlet

Argon gas outlet

Water cooling coil

Inconel vessel

Vertical furnace

O_2^- gases

Graphene oxides cathode

oxide ions

Graphene oxides anode

Molten KOH
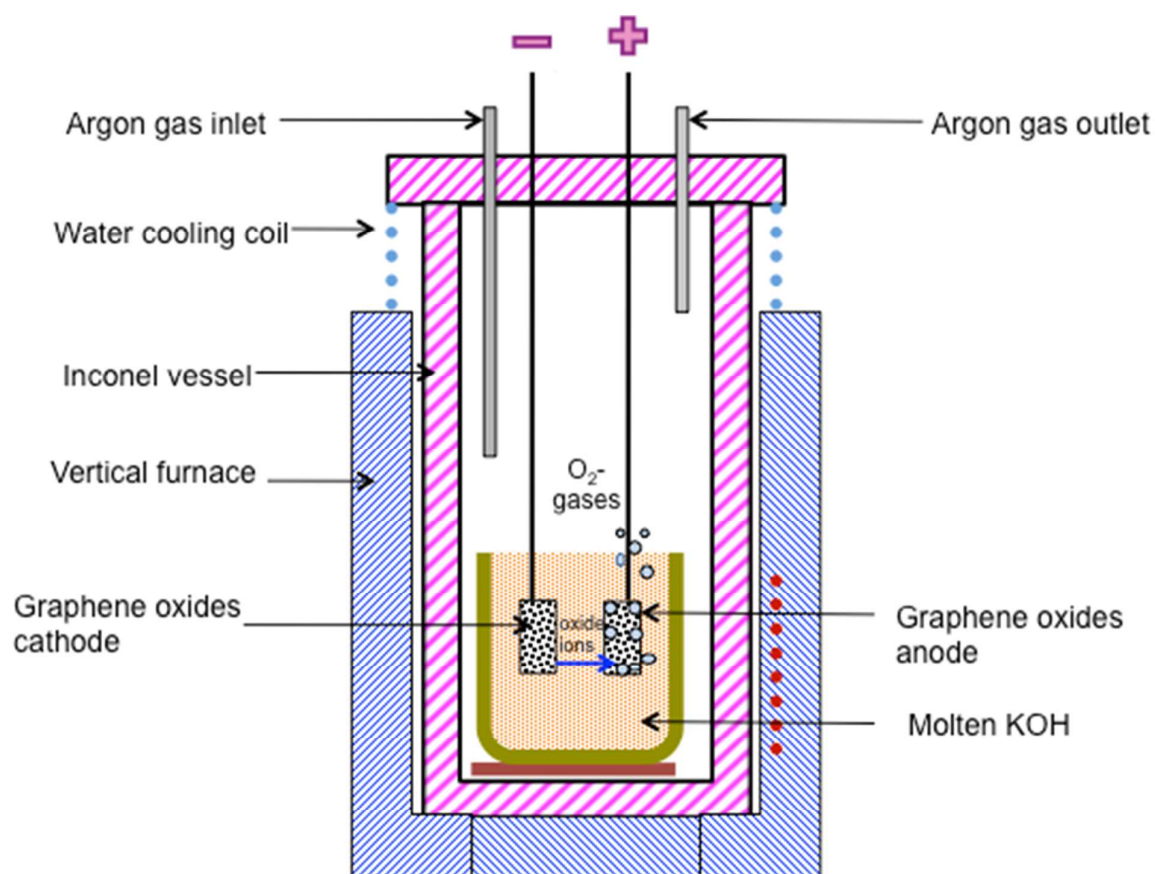
Figure S5. The molten salts reactor used for the electrochemical activation process.

Calculating the specific capacitance obtained from CV and charge-discharge curves

From charge-discharge measurements, the specific capacitances of the rGO were obtained from the acquired data using following equation:

$$C = 4I\Delta t / m\Delta V \qquad (1)$$

Where C represents the specific capacitances, I the constant charge current, Δt for the discharging period, m for the mass of graphene used as electrodes, ΔV for the voltage of capacitor after constant current charging.

From CV curves, the specific capacitances were calculated according to the following equation:

$$C = (\int I dV)/(vmV) \qquad (2)$$

Where I represents the current density during charging-discharging, V is the potential, v is the potential scanning rate, and m is the mass of the graphene electrodes.

Calculating the electrosorption capacity:

The electrosorption capacity (Q) of the electrode was calculated from the following equation:

$$Q = \frac{(C_o - C)V}{m} \qquad (3)$$

Where C_0 and C (mg/L) were the initial and equilibrium concentration of NaCl, respectively. V was the volume of the NaCl solution in the CDI device, and m was the total mass loading of the active material ECAG.

The charge efficiency Λ was calculated from the equation:

$$\Lambda = Q/\Sigma \qquad (4)$$

Where Q is the electrosorption capacity calculated at equilibrium (at the point of minimum conductivity in the outlet stream and Σ is the equilibrium charge, $\Sigma = \int I dt$.

Table S1. Comparison of the electrochemical performance of rGO supercapacitor electrodes from different reduction method

Process	C/O ratio	Electrical conductivity (S/m)	Specific Capacitance (F/g)	Specific surface area (m^2/g)	Specific capacitance Retention %
Reduction by microwave irradiation then activated by KOH.[1]	35	500 (Pressed Powder)	200 ionic liquid	3100 (activated)	97 after 10000 cycles
Reduction by hydrazine at 100 ^{o}C.[2]	11.5	200 (Pressed Powder)	135 KOH	705	Unknown
Reduction with Hydrazine vapor at low pressure.[3]	7.3	100 Film	205 KOH	320	90 after 1200 cycles
Thermal reduction at 200 ^{o}C under high vacuum (below 1 Pa).[4]	10	Unknown	122 KOH	350	~ 94 after 100 cycles
Solvothermal reduction in propylene carbonate at 150 ^{o}C.[5]	8.3	2100 (Paper-like)	120 Organic	Unknown	Unknown
Reduction with hydrobromic acid at 110 ^{o}C.[6]	3.9	0.023	348 in H_2SO_4 and 158 in ionic liquid (pseudocapacitance involved)	Unknown	Increased to 125 % after 1800 cycle
Thermal reduction at 1050 ^{o}C.[7]	10^8	2300 (Pressed powder)[8]	117 H_2SO_4	925	Unknown
Solvothermal reduction in DMF at 150 ^{o}C.[9]	5.97	Unknown	276 H_2SO_4 (pseudocapacitance involved)	Unknown	Increased to 106 % after 1980 cycles
Reduction with urea at 95 ^{o}C.[10]	4.5	43 (Paper-like)	255 H_2SO_4 (pseudocapacitance involved)	590	93% after 1200 cycles
Reduction with urea at 95 ^{o}C followed by annealing at 800 ^{o}C under nitrogen.[10]	19.7	4520 (Annealed paper)	172 H_2SO_4	630	94% after 1200 cycle
Hydrothermal reduction with sodium ascorbate at 95 ^{o}C.[11]	10.3	1 (hydrogel)	190 H_2SO_4[12] 186 solid state	414	93.6 after 10000 cycles
Reduction by laser irradiation.[13]		1738 (film)	204 solid state	1520	95% after 1000 cycles
Electrochemical reduction in molten salt.[14]	12.5	2300 (membrane)	255 KOH	565	95% after 5000 cycles
Reduction by Li in molten LiCl-KCl at 370 ^{o}C.[15]	7	2400 (paper-like)	203 KOH	320	97% after 2000 cycles

Table S2. Salt electrosorption performance reported for different carbon materials as electrodes for CDI.

Carbon Materials	Initial Concentration (mg/ml)	Electrosorption capacity(mg/g)	Time until equilibrium (min)	Electrosorption rate(mg/g.min)	Charge efficiency	Flow rate (mL/min)	Cell potential (V)	Ref
Activated Carbon	1000	5.9	~7		0.53	3	1.6	16
rGO/activated carbon	50	0.8	~60	0.12	0.24	25	2	17
Activated Carbon/QPVP	500	20.6	~10	1	0.68	8.67	1.2	18
Activated carbon cloth/ZnO	1000	7.7	~6		0.78	3	1.6	16
Amine Modified Microporous Carbon	250	5.3	~60		0.53	20	1.1	19
Amine and carboxylic group modified graphene	300	18.43	~10		0.87	20	1.4	20
Sulfonic and amine functionalised graphene	500	13.72	~80	0.12	0.85	40	1.4	21
Graphene-like nanoflakes	25	1.3	> 40			45	2	22
Graphene-CNT	29	1.4	~120			25	2	23
Graphene aerogel/TiO_2	500	15.1	~6		0.68	30	1.2	24
Activated 3D graphene	70	11.86	~25			10	2	25
Sulfonated graphene-carbon nanofibers	100	9.54	~65		0.43	5	1.6	26
Sponge templated graphene	52	4.95	~60			3	1.5	27
Porous Carbon Rods	1000	16.2	~40			27	1.2	28
Graphene-coated carbon spheres	29	2.3	~120			25	1.6	29
Cellulose Derived Graphenic Fibers	500	13.1	~90-120				1.2	30
3-D macroporous graphene	52	5.93	~50			25	2	31

The equilibrium is defined as the point where the conductivity of the outlet stream stopped decreasing and started to increase.

References:

(1)   Zhu, Y.; Murali, S.; Stoller, M. D.; Ganesh, K. J.; Cai, W.; Ferreira, P. J.; Pirkle, A.; Wallace, R. M.; Cychosz, K. A.; Thommes, M.; Su, D.; Stach, E. A.; Ruoff, R. S. Carbon-Based Supercapacitors Produced by Activation of Graphene, *Science* **2011**, *332*, 1537-1541.

(2)   Stoller, M. D.; Park, S.; Yanwu, Z.; An, J.; Ruoff, R. S. Graphene-Based ultracapacitors, *Nano Letters* **2008**, *8*, 3498-3502.

(3)   Wang, Y.; Shi, Z. Q.; Huang, Y.; Ma, Y. F.; Wang, C. Y.; Chen, M. M.; Chen, Y. S. Supercapacitor Devices Based on Graphene Materials, *J. Phys. Chem. C* **2009**, *113*, 13103-13107.

(4)   Lv, W.; Tang, D. M.; He, Y. B.; You, C. H.; Shi, Z. Q.; Chen, X. C.; Chen, C. M.; Hou, P. X.; Liu, C.; Yang, Q. H. Low-Temperature Exfoliated Graphenes: Vacuum-Promoted Exfoliation and Electrochemical Energy Storage, *Acs Nano* **2009**, *3*, 3730-3736.

(5)   Zhu, Y. W.; Stoller, M. D.; Cai, W. W.; Velamakanni, A.; Piner, R. D.; Chen, D.; Ruoff, R. S. Exfoliation of Graphite Oxide in Propylene Carbonate and Thermal Reduction of the Resulting Graphene Oxide Platelets, *Acs Nano* **2010**, *4*, 1227-1233.

(6)   Chen, Y.; Zhang, X.; Zhang, D.; Yu, P.; Ma, Y. High Performance Supercapacitors Based on Reduced Graphene Oxide in Aqueous and Ionic Liquid Electrolytes, *Carbon* **2011**, *49*, 573-580.

(7)   Vivekchand, S. R. C.; Rout, C. S.; Subrahmanyam, K. S.; Govindaraj, A.; Rao, C. N. R. Graphene-Based Electrochemical Supercapacitors, *J. Chem. Sci.* **2008**, *120*, 9-13.

(8)   Schniepp, H. C.; Li, J.-L.; McAllister, M. J.; Sai, H.; Herrera-Alonso, M.; Adamson, D. H.; Prud'homme, R. K.; Car, R.; Saville, D. A.; Aksay, I. A. Functionalized Single Graphene Sheets Derived from Splitting Graphite Oxide, *The Journal of Physical Chemistry B* **2006**, *110*, 8535-8539.

(9)   Lin, Z.; Liu, Y.; Yao, Y.; Hildreth, O. J.; Li, Z.; Moon, K.; Wong, C.-p. Superior Capacitance of Functionalized Graphene, *The Journal of Physical Chemistry C* **2011**, *115*, 7120-7125.

(10)   Lei, Z.; Lu, L.; Zhao, X. S. The Electrocapacitive Properties of Graphene Oxide Reduced by Urea, *Energy & Environmental Science* **2012**, *5*, 6391-6399.

(11)   Sheng, K.-x.; Xu, Y.-x.; Li, C.; Shi, G.-q. High-Performance Self-Assembled Graphene Hydrogels Prepared by Chemical Reduction of Graphene Oxide, *New Carbon Materials* **2011**, *26*, 9-15.

(12)   Xu, Y.; Lin, Z.; Huang, X.; Liu, Y.; Huang, Y.; Duan, X. Flexible Solid-State Supercapacitors Based on Three-Dimensional Graphene Hydrogel Films, *ACS Nano* **2013**, *7*, 4042-4049.

(13)   El-Kady, M. F.; Strong, V.; Dubin, S.; Kaner, R. B. Laser Scribing of High-Performance and Flexible Graphene-Based Electrochemical Capacitors, *Science* **2012**, *335*, 1326-1330.

(14)   Abdelkader, A. M. Electrochemical synthesis of highly corrugated graphene sheets for high performance supercapacitors, *Journal of Materials Chemistry A* **2015**, *3*, 8519-8525.

(15)   Abdelkader, A. M.; Vallés, C.; Cooper, A. J.; Kinloch, I. A.; Dryfe, R. A. W. Alkali reduction of graphene oxide in molten halide salts: Production of corrugated graphene derivatives for high-performance supercapacitors, *ACS Nano* **2014**, *8*, 11225-11233.

(16)   Laxman, K.; Myint, M. T. Z.; Khan, R.; Pervez, T.; Dutta, J. Improved desalination by zinc oxide nanorod induced electric field enhancement in capacitive deionization of brackish water, *Desalination* **2015**, *359*, 64-70.

(17)   Li, H.; Pan, L.; Nie, C.; Liu, Y.; Sun, Z. Reduced graphene oxide and activated carbon composites for capacitive deionization, *Journal of Materials Chemistry* **2012**, *22*, 15556-15561.

(18)   Wu, T.; Wang, G.; Zhan, F.; Dong, Q.; Ren, Q.; Wang, J.; Qiu, J. Surface-treated carbon electrodes with modified potential of zero charge for capacitive deionization, *Water Research* **2016**, *93*, 30-37.

(19)   Gao, X.; Omosebi, A.; Landon, J.; Liu, K. Enhanced Salt Removal in an Inverted Capacitive Deionization Cell Using Amine Modified Microporous Carbon Cathodes, *Environmental Science & Technology* **2015**, *49*, 10920-10926.

(20)   El-Deen, A. G.; Boom, R. M.; Kim, H. Y.; Duan, H.; Chan-Park, M. B.; Choi, J.-H. Flexible 3D Nanoporous Graphene for Desalination and Bio-decontamination of Brackish Water via Asymmetric Capacitive Deionization, *ACS Applied Materials & Interfaces* **2016**, *8*, 25313-25325.

(21)   Liu, P.; Wang, H.; Yan, T.; Zhang, J.; Shi, L.; Zhang, D. Grafting sulfonic and amine functional groups on 3D graphene for improved capacitive deionization, *Journal of Materials Chemistry A* **2016**, *4*, 5303-5313.

(22)   Li, H.; Zou, L.; Pan, L.; Sun, Z. Novel Graphene-Like Electrodes for Capacitive Deionization, *Environmental Science & Technology* **2010**, *44*, 8692-8697.

(23)   Zhang, D.; Yan, T.; Shi, L.; Peng, Z.; Wen, X.; Zhang, J. Enhanced capacitive deionization performance of graphene/carbon nanotube composites, *Journal of Materials Chemistry* **2012**, *22*, 14696-14704.

(24)   Yin, H.; Zhao, S.; Wan, J.; Tang, H.; Chang, L.; He, L.; Zhao, H.; Gao, Y.; Tang, Z. Three-Dimensional Graphene/Metal Oxide Nanoparticle Hybrids for High-Performance Capacitive Deionization of Saline Water, *Advanced Materials* **2013**, *25*, 6270-6276.

(25)   Li, Z.; Song, B.; Wu, Z.; Lin, Z.; Yao, Y.; Moon, K.-S.; Wong, C. P. 3D porous graphene with ultrahigh surface area for microscale capacitive deionization, *Nano Energy* **2015**, *11*, 711-718.

(26)   Qian, B.; Wang, G.; Ling, Z.; Dong, Q.; Wu, T.; Zhang, X.; Qiu, J. Sulfonated Graphene as Cation-Selective Coating: A New Strategy for High-Performance Membrane Capacitive Deionization, *Advanced Materials Interfaces* **2015**, *2*, 1500372-n/a.

(27)   Yang, Z. Y.; Jin, L. J.; Lu, G. Q.; Xiao, Q. Q.; Zhang, Y. X.; Jing, L.; Zhang, X. X.; Yan, Y. M.; Sun, K. N. Sponge-templated preparation of high surface area graphene with ultrahigh capacitive deionization performance, *Advanced Functional Materials* **2014**, *24*, 3917-3925.

(28)   Xu, X.; Li, J.; Wang, M.; Liu, Y.; Lu, T.; Pan, L. Shuttle-like Porous Carbon Rods from Carbonized Metal–Organic Frameworks for High-Performance Capacitive Deionization, *ChemElectroChem* **2016**, *3*, 993-998.

(29)   Wang, H.; Shi, L.; Yan, T.; Zhang, J.; Zhong, Q.; Zhang, D. Design of graphene-coated hollow mesoporous carbon spheres as high performance electrodes for capacitive deionization, *Journal of Materials Chemistry A* **2014**, *2*, 4739-4750.

(30)   Pugazhenthiran, N.; Sen Gupta, S.; Prabhath, A.; Manikandan, M.; Swathy, J. R.; Raman, V. K.; Pradeep, T. Cellulose Derived Graphenic Fibers for Capacitive Desalination of Brackish Water, *ACS Applied Materials & Interfaces* **2015**, *7*, 20156-20163.

(31)   Wang, H.; Zhang, D.; Yan, T.; Wen, X.; Zhang, J.; Shi, L.; Zhong, Q. Three-dimensional macroporous graphene architectures as high performance electrodes for capacitive deionization, *Journal of Materials Chemistry A* **2013**, *1*, 11778-11789.